3-Dimensional Carbon Nanotube-Graphene Structure for Flexible Li-ion Battery

C.W. Kang*, R Baskaran*, P. Mumukshu*, W.B. Choi*

*Department of Materials Science and Engineering, University of North Texas, North Texas Discovery Park, 3940 North Elm St. Suite E-132, Denton, TX 76207, USA

ABSTRACT

The intensive research on the flexible Li-ion battery has been recently conducted in order to provide next generation flexible electronic devices with required high power and energy. We have presented a new architecture of 3-dimensioanl (3D) carbon nanotube-graphene on flexible polyethylene terephthalate (PET) film by chemical vapor deposition and a simple lamination process. The flexible 3D anode revealed excellent electrochemical performance obtained by a half-cell and good electronic conductivity under repeated bending test. According to the outstanding results, we assembled a flexible Li-ion battery based on the 3D architecture. It is believed that the flexible Li-ion battery based on the nanomaterial architecture can be used as one of the strong candidates for next generation flexible energy storage devices.

Keywords: 3 dimensional anode, flexible Li-ion battery, carbon nanotubes, graphene, polyethylene terephthalate (PET)

INTRODUCTION

It has been a current status to find the diverse flexible electronic devices such as foldable smart phones, roll-up displays, and active radio frequency identification (RFID) tags in the market. Li-ion battery (hereafter referred to as LIB) has been mainly investigated as a significant energy storage device for the flexible electronics [1-2]. To follow the social demand, many worldwide research groups have developed diverse flexible LIB cells and demonstrated excellent electrochemical performance of the cells. CNT-cellulose paper based flexible nanocomposite thin-film anodes were fabricated and the cell comprising the anodes showed a reversible capacity around 110 $mAhg^{-1}$ during a few cycles [3]. Chemical vapor deposition (CVD) grown CNT-carbon layer composite anodes were prepared for a paper LIB and the anode based cell showed the highly stable reversible capacity of 572 $mAhg^{-1}$ after 100 cycles [4]. Despite such excellent results, they showed limitations such as the low loading density of carbon based nanomaterials and the requirement of complicated synthesis process. Also, next generation flexible LIB needs the high specific and volumetric capacities of the anodes upon being mechanically flexed. Such requirement has been driven the development of novel flexible LIB anodes without heavy and mechanically deformed metallic current collectors or even polymer substrates [5].

As electric vehicles have been greatly attracted and recently commercialized, the nanomaterial based anodes have been intensively explored. Among the strong candidate materials, carbon nanotubes [6], silicon nanowires [7], and transitional metal oxide nanoparticles [8] have been employed since they possess inherently designed properties such as short diffusion length of lithium ions, high specific surface area, and mechanical resilience against lithiation/delithiation cycling. In our team, we demonstrated high capacity and excellent stability of LIB anode using interface-controlled binder-fee multiwall carbon nanotubes (hereafter referred to as MWCNTs) grown on copper foil by a CVD method [9]. Nevertheless, the carbon nanostructure based anode materials have a drawback which is the low volumetric loading density and capacity [10]. To address the issue, many research teams have focused on the 3 dimensional (3D) architecture of anode materials through introducing 3D metal current collectors. Electrodeposited active materials were obtained after the removal of template and the electro-polishing of nickel and a pouch-type LIB cell constituted by an MnO_2 cathode and a graphite anode showed the specific capacity of around 110 $mAhg^{-1}$ even at 60C charge and discharge rate [11].

In this paper, we would like to propose a novel architecture which is 3D MWCNTs-graphene transferred onto flexible PET film for the enhanced performance of flexible LIB anode. 3D MWCNTs were grown on Cu mesh through a catalytic thermal CVD method and transferred over graphene-PET film, serving as both active materials and current collectors for LIB anode. Also, graphene interfacial layer played a significant role in promoting electronic conductivity for the 3D MWCNT network structure.

EXPERIMENT

As a core current collector, Cu mesh (200 Mesh Copper, TWP) was adjusted with the overall thickness 50 μm and hole size 65 μm. 3D MWCNTs were grown by a two-step process which is done by the sputter deposition of Ti as a carbon diffusion barrier layer and Ni as a catalytic thin layer onto Cu mesh and the decomposition of ethylene (C_2H_4) precursor gas flowed with hydrogen (H_2) carrier gas (1:2 volume ratio of C_2H_4 to H_2) at the growth temperature 750°C for 50 minutes. As proved in the high resolution transmission

electron microscopy (HRTEM) in our previous publication, TiC layer was formed between MWCNTs and Cu and it played an important role in improving electrical conductivity and bonding strength [9].

Thermal lamination process is essential to transfer 3D MWCNTs grown on Cu mesh onto graphene laminated polyethylene terephthalate (PET) flexible substrate. The processing flows for the transferring of graphene onto PET film and 3D MWCNTs onto graphene-PET film were shown in our previous reports, respectively [12-13]. The as-prepared 3D MWCNTs/Cu mesh was attached to graphene/PET film in a "face-to-face" orientation and the sandwiched samples were thermally laminated at around 70°C, resulting in the strongly adhered structure of 3D MWCNTs-graphene to PET film. Fig. 1 (g) demonstrates a digital image of the high flexibility of the structure. Structural properties of the as-prepared 3D MWCNTs-graphene-PET structures were discovered using a field emission scanning electron microscope (FESEM) (JEOL, JSM-7000F; HITACHI, S-4800) and an energy dispersive spectroscope (EDS) (Thermo Electron Corporation, NORAN System SIX). Electron conductivity of the structure was measured using a four-probe station (MS Tech, Korea) controlled by a digital multimeter (Keithley, 2400). The values of sheet resistance were recorded after flexing the samples at the different bending angles from 0° to 180° with 30° intervals.

For the charge-discharge cycling test, the coin cell (CR 2032) was assembled in the inert glove box with the extremely low level of humidity (less than 1.0 ppm) and oxygen (less than 1.0 ppm). Our proposed 3D MWCNTs-graphene-PET structure was used as a working electrode, while Li metal was used as both counter and reference electrodes (a half-cell). To enhance the electronic conductivity between the working electrode and the stainless steel bottom cap of the coin cell, a crescent-shape Cu foil was placed on the working electrode and the cap to act as an electronic pathway, which was impossible for insulating PET film to be obtained. 1 M solution of $LiPF_6$ lithium salt dissolved into 1:1 (v/v) mixture solvent of ethylene carbonate (EC) and dimethylene carbonate (DMC) was used as electrolyte (Soulbrain Inc.). Polypropylene (PP) material (Separator 2400) was used as separator. With assembled and crimped coin cells, the charge-discharge cycle performance was conducted using a battery tester (MACCOR Inc.) at room temperature under various current densities.

DISCUSSION

It is the structural properties of the anode materials that significantly affect the electrochemical performance of LIB cells. As seen in Fig. 1(a), the 3D MWCNTs have the array of the regularly distanced and patterned square-looking structures, which were successfully transferred over the graphene on PET film. From EDS analysis done by arbitrary sites of the 3D MWCNTs on graphene-PET film, higher than 99 atom% of carbon and less than 0.2 atom% of copper were detected (see Fig. 1(b)). Fig. 1(c) demonstrated the magnified SEM plane view of the transferred 3D MWCNTs over PET film. As seen in the SEM image, the darker regions (in contrast to the brighter box regions) were stemmed from the bottom side of the densely packed 3D MWCNTs directly grown on the original Cu mesh substrate. Once being pressed by a thermal laminator, the MWCNTs in the upper region were filled into the free spaces (It is understood that the brighter box regions in the SEM image were matched with the holes in the original Cu mesh.). As shown in Fig. 1(d), the 3D MWCNTs with the average height around 40 μm were strongly adhered to the PET film through the pressure-sensitive adhesion layer coated on the commercial PET film. During thermal lamination process, the layer served as a glue to strongly bond between MWCNTs and graphene on PET film. Fig. 1(d) demonstrated that the glue layer appeared in accordance with the contact area of the transferred MWCNTs. Moreover, a cross-sectional schematic diagram indicated the key components as well as white colored pseudo-sinusoidal conformation curve representing the glue layer (see Fig. 1(e)). The graphene layer between 3D MWCNTs and PET film was very thin (approximately 1-3 layer). The overall thickness of the pressure-sensitive adhesive was thicker than that of the graphene layer; as a result, the adhesive could penetrate the defects and grain boundaries of graphene layer and then, make 3D MWCNT based patterned structure strongly bond to PET substrate. Nevertheless, the graphene layer played an important role in maintaining structural integrity and Ohmic junction of the interface. The morphological characteristics of the 3D MWCNTs can be described as the randomly oriented growth with the diameters in the range of 200 nm to 300 nm as shown in Fig. 1(f). In terms of optical property (data not shown), it is implied that the higher areal mass density of MWCNTs may increase the amount of the filled MWCNTs into the hole spaces, decreasing the optical transparency of the 3D MWCNTs-graphene-PET structure. The areal density of the structure was in the range between 0.65 and 1.75 mg/cm^2.

As another important issue, PET based insulating substrates inherently have the limitation of poor electronic conductivity. Therefore, 3D MWCNTs are expected to be electronically conductive materials beside electrochemically active materials. From sheet resistance measurement, it was discovered that 3D MWCNT networks showed high electric conductivity with low sheet resistance

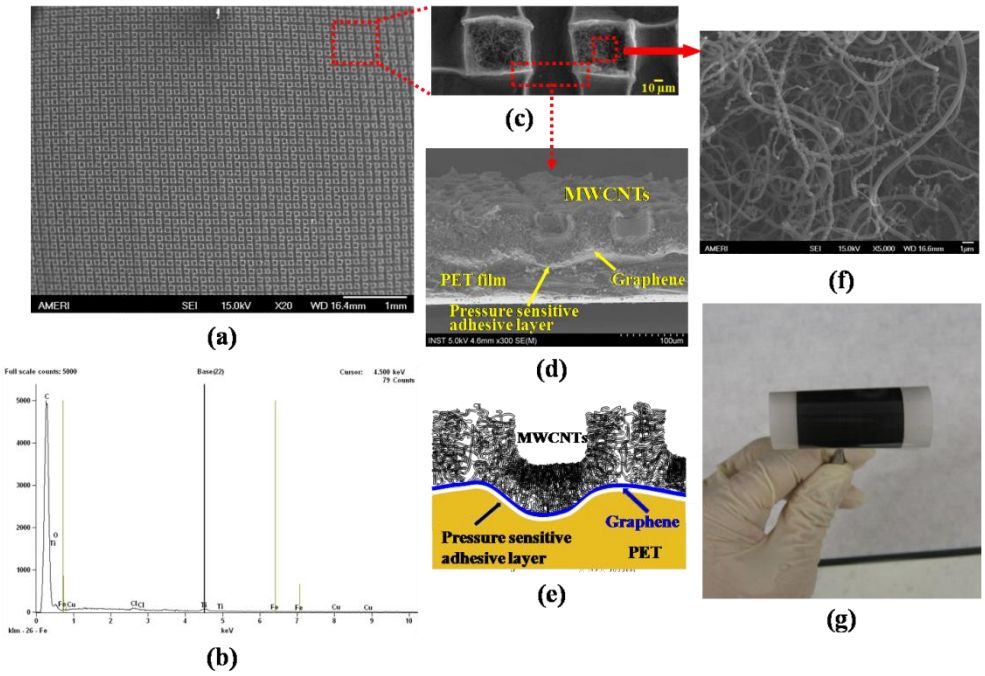

Figure 1: Structural characterization of as-prepared 3D MWCNTs-graphene-PET architecture. (a) The SEM plane view of large area 3D MWCNTs-graphene-PET film, (b) EDS spectra of a spot of 3D MWCNTs, which was transferred onto graphene-PET film, composed of higher than 99 atom% of carbon and less than 0.2 atom% of copper, (c) The zoomed-in and (d) The cross-sectional SEM images of 3D MWCNTs-graphene-PET structure, (e) Schematic diagram (not to scale) of the cross-sectional image presented in Fig. 1(d), (f) The magnified SEM image of the randomly oriented grown MWCNTs, (g) The digital image showing the high flexibility of 3D MWCNTs-graphene-PET structure.

~95 Ω/sq (data not shown), which was higher than ~40-50 Ω/sq gained from the SWCNTs spray coated on PET substrates [14]. Furthermore, true potential as flexible LIB anodes could be confirmed by constant electronic conductivity after repeated bending tests. For the characterization technique, the sheet resistance measurement of the 3D MWCNTs-graphene-PET structure was proceeded as a function of bending angle. As a result, even at the bending angle around 180°, the normalized sheet resistance (defined as the sheet resistance measured at a bending angle divided by the sheet resistance measured at a zero degree bending angle, (R_{deg}/R_o)) was around one (data not shown). Such structural integrity and good electrical property are mainly attributed to not only the strong bonding of MWCNTs and graphene to PET film but also the authentic macroscopic, pliable, and porous nature of the 3D MWCNT structure, which are suited to relieve the bending stress.

Utilizing the structural and electrical properties of 3D MWCNTs-graphene-PET mentioned in the previous section, the LIB performance of the structure was found through charge-discharge cycles with the half-cell. As seen in Fig. 2(a), the initial lithiation and delithiation profile was created at the current density of 63 mAg^{-1} (0.17C). The lithiation and delithiation capacities were reached up to 293 $mAhg^{-1}$ ($LiC_{7.6}$) and 153 $mAhg^{-1}$ ($LiC_{14.6}$), respectively. The values of the specific capacities were lower than those obtained by 3D MWCNTs on Cu mesh anode based cells [15]. The finding may imply that there is no contribution of PET with insulating nature as a current collector. On the contrary, the values were higher than the reversible capacity (110 $mAhg^{-1}$) achieved by the flexible LIB cell comprising a CNT-cellulose paper anode [3]. It is recalled that the 3D MWCNTs as anode materials showing the low sheet resistance (95Ω/sq) could mainly serve as active materials for the electrochemical redox reactions by determining electron charge and lithium ion transfer rates in the MWCNT networks. Similar to the previous reports, the higher irreversibility (around 50%) may be due to the electrolyte decomposition and the subsequent solid electrolyte interface (SEI) formation on the surface of MWCNTs occurred around at 0.8V, showing a plateau region in Fig. 2(a). (The phenomenon reflects one of the drawbacks of carbon based anode materials combined with liquid electrolytes during LIB test.) [16-17]. Different from the previous report, in our case, the graphene layer lying between 3D MWCNTs and PET film was too thin and light to be regarded as true electrochemical active material [18]. It was emphasized that higher reversible, stable specific capacity around 124 $mAhg^{-1}$ until the 50th cycle was attained even at the higher current density 1.7C (632 mAg^{-1}), compared to that from the recently published flexible

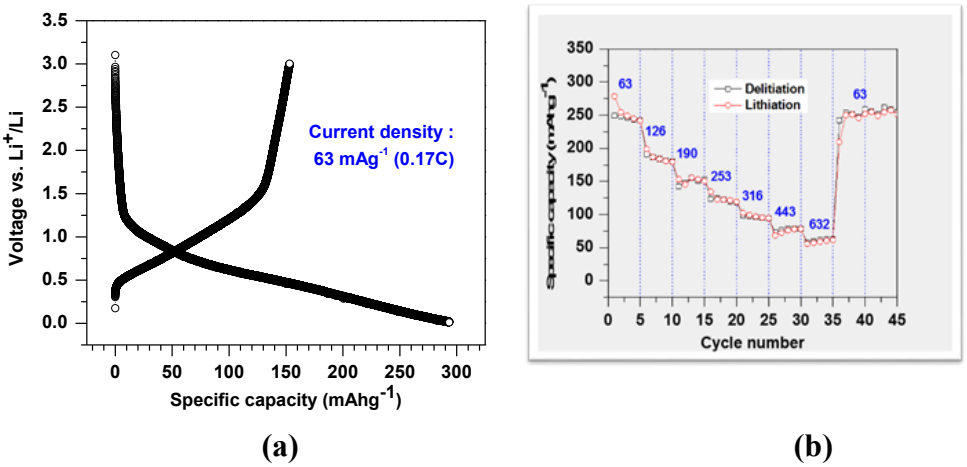

(a) **(b)**

Figure 2: Electrochemical performance of the 3D MWCNTs-graphene-PET as a flexible LIB anode architecture. (a) Primary galvanostatic charge and discharge profiles of the anode, (b) Cycling performance of the anode. Numerical values indicate the applied current densities during the characterization.

LIB cell with CNT-cellulose paper anode (e.g. 110 $mAhg^{-1}$ at 10 mAg^{-1}) [3]. As one of the reasons for the good result, non-aqueous electrolyte (e.g. lithium salt dissolved into a mixture solvent of alkyl carbonates) could effectively penetrate into and spread over the 3D MWCNTs' structures so that the conductivity of lithium ions could be facilely inserted and extracted into and from the structures [19]. Also, the 3D MWCNTs and graphene architecture maintained excellent structural integrity under the repeated cycling because of the pressure-sensitive adhesive layer.

CONCLUSIONS

We have demonstrated the fabrication of 3D MWCNTs-graphene-PET as an anode for flexible LIB and its electrochemical performance. The regular and repetitive array of 3D MWCNT pattern in the large area sustained structural integrity and demonstrated high electronic conductivity (low sheet resistance (~95 Ω/sq)) under severe bending test. The assembled Li-ion button cell comprising the architecture showed excellent charge-discharge cycling stability with high reversible specific capacity ~250 $mAhg^{-1}$. Considering all the features, it is anticipated that the flexible 3D MWCNTs-graphene-PET structure can be used as a key anode for next generation flexible Li-ion batteries.

REFERENCES

[1] L. Hu and Y. Cui, Energy Environ Sci, 5, 6423, 2012.
[2] L Hu, H. Wu, F. L. Mantia, Y. Yang and Y. Cui, ACS Nano, 4, 5843, 2010.
[3] V. L. Pushparaj, M. M. Shaijumon, A. Kumar, S. Murugesan, L. Ci and R. Vajtai, Proc Natl Acad Sci, 104, 13574, 2007.
[4] J. Chen, A. I. Minett, Y. Liu, C. Lynam, P. Sherrell and C. Wang, Adv Mater 20, 566, 2008.
[5] L. Hu, J. W. Choi, Y. Yang, S. Jeong, F. L. Mantia and L. F. Cui, Proc Natl Acad Sci 2009;106(51):21490–4.
[6] X. X Wang, J. N. Wang, H. Chang and Y. F. Zhang, Adv Funct Mater, 17, 3613, 2007.
[7] C. K. Chan, R. Ruffo, S. Hong, R. A. Huggins and Y. Cui, J Power Sources 189, 34, 2007.
[8] P. Poizot, S. Laruelle, S. Grugeon, L. Dupont and J. M. Tarascon, Nature 407, 496, 2000.
[9] I. Lahiri, S. W. Oh, J. Y. Hwang, S. J. Cho, Y. K. Sun and R. Banerjee, ACS Nano, 4, 3440, 2010.
[10] Y. Gogotsi and P. Simon, Science 34, 6058, 2011.
[11] H. Zhang, X. Yu and P. V. Braun, Nat Nanotechnol, 6, 277, 2011.
[12] V. P. Verma, S. Das, I. Lahiri and W. B. Choi, Appl Phys Lett, 96, 203108, 2010.
[13] C. W. Kang, R. Baskaran, J. Y. Hwang, B. C. Ku and W. B. Choi, Carbon, 68, 493, 2014.
[14] M. Kaempgen, C. K. Chan, J. Ma, Y. Cui and G. Gruner, Nano Lett, 9, 1872, 2009.
[15] C. Kang, I. Lahiri, R. Baskaran, W. G. Kim, Y. K. Sun and W. B. Choi, J Power Sources, 219, 364, 2012.
[16] C. D. L. Casas and W. Li, J Power Sources, 208, 74, 2012.
[17] M. Winter, K. C. Moeller and J. O. Besenhard, "Carbonaceous and graphitic anodes. In: Nazri GA, Pistoia G, editors. Lithium batteries: science and technology," New York: Springer, 144-194, 2004.
[18] M. Liang and L. Zhi, J Mater Chem, 19, 5871, 2009.
[19] D. Aurbach and A. Schechter, "Advanced Liquid Electrolyte Solutions. In: Nazri GA, Pistoia G, editors. Lithium batteries: science and technology," New York: Springer, 530-573, 2004.